CellPress

Current Biology
Review

Growth and Development of Three-Dimensional Plant Form

Christopher D. Whitewoods and Enrico Coen*
Department of Cell and Developmental Biology, John Innes Centre, Colney Lane, Norwich, NR4 7UH, UK
*Correspondence: enrico.coen@jic.ac.uk
http://dx.doi.org/10.1016/j.cub.2017.05.079

Plants can generate a spectacular array of complex shapes, many of which exhibit elaborate curvature in three dimensions, illustrated for example by orchid flowers and pitcher-plant traps. All of these structures arise through differential growth. Recent findings provide fresh mechanistic insights into how regional cell behaviours may lead to tissue deformations, including anisotropies and curvatures, which shape growing volumes and sheets of cells. Here were review our current understanding of how genes, growth, mechanics, and evolution interact to generate diverse structures. We illustrate problems and approaches with the complex three-dimensional trap of the bladderwort, *Utricularia gibba*, to show how a multidisciplinary approach can be extended to new model systems to understand how diverse plant shapes can develop and evolve.

Introduction

From the lips, domes and spurs of orchid flowers to the insect-trapping cups of carnivorous plants, plants produce an incredible diversity of three-dimensional shapes. Many of these structures can be viewed as adaptations to manipulate animals: nectar tubes select pollinators with probosces of particular lengths; tightly closed floral lips reserve entry for bees; and the air-tight seal of a bladderwort trap's mouth captures small animals at the press of a trigger hair.

All of these shapes begin as small groups of cells that transform themselves, through growth, into the final form. A key problem is how genes modulate cell behaviours to achieve such transformations. Here we review our current understanding and approaches to this problem based on current experimental systems, and use the bladderwort *Utricularia* trap — a hollow structure that traps small invertebrates through suction (Figure 1E) — to illustrate how key principles may be extended and further explored with new model systems. We consider two types of tissue configuration: a *volume*, in which dimensions along the three axes of the tissue are comparable; and a *sheet*, where dimensions along one axis (thickness) is much smaller than the other two. These are two ends of a continuum, but provide a useful distinction for modelling shape change.

Many plant structures begin as volumes and become progressively more sheet-like. The early *Utricularia* trap primordium, for example, is around 30 μm in each dimension (Figure 1A). It then undergoes an invagination to produce a simple cup (Figure 1B). At this stage, the trap may be considered as a curved sheet. This sheet could correspond either to a single layer of cells folded on itself (the sheet is a monolayer, one cell thick; Figure 1B, green line) or to the walls of the cup (the sheet is multilayer, two cell layers thick; Figure 1B, orange line). As the trap grows, further folds are generated (for example, the trap door, Figure 1C,D, red) and the tissue broadens in some regions (threshold, Figure 1D, blue). The transition from a primordial volume to a sheet-like form is typical of other plant organs, such as leaves or petals, although unlike the trap the multilayer sheets are typically 6–8 cell layers thick. In all cases, the final shape reflects the pattern of folds and curvature generated through growth. This raises the question of how we define and measure growth.

What Is Growth?

As the early trap grows, two processes occur concurrently: an increase in organ size and an increase in cell number through division. Here we use growth to refer to irreversible increase in size. This definition can be applied at any scale, from the enlargement of individual cells, to groups of cells or entire tissues. Division refers to the partitioning of cells and introduction of new cell walls, which may occur while a tissue grows. The combination of division and growth leads to cells with particular sizes and shapes, such as the spherical, rectangular and trapezoid cells in the *Utricularia* trap (Figure 1F,G,H).

How can we describe growth mathematically? If growth is equal in all directions (isotropic), and uniform across a structure, the structure increases in size without changing shape. Growth can then be summarised by a single number: the growth rate of the tissue, denoted by a scalar (Figure 2A). If growth is isotropic but its rate varies from one position to another, we need a field of scalars to describe growth — the growth rate at each position (Figure 2B).

If growth is not equal in all directions (anisotropic), a scalar field is no longer sufficient to represent growth. Perhaps growth then corresponds to a vector. As well as magnitude, a vector has both an axis (orientation) and sense (an arrowhead on one end only). A growing tissue can be described as a field of vectors, each vector corresponding to the velocity at which points move as the tissue grows (velocity field; Figure 2A,C). For example, with *Utricularia* we could consider each of the cell wall vertices shown in Figure 1A as points or landmarks that are displaced through growth with particular velocities. Indeed, this approach has been used to analyse growth [1]. However, the velocity field depends on the point of reference and is not a direct read-out of local growth rates. For example, if you superimpose two growth stages of *Utricularia* and align the base of the trap, points near the mouth will have higher velocities than points near the base, whereas if you align the mouths, points at the base will

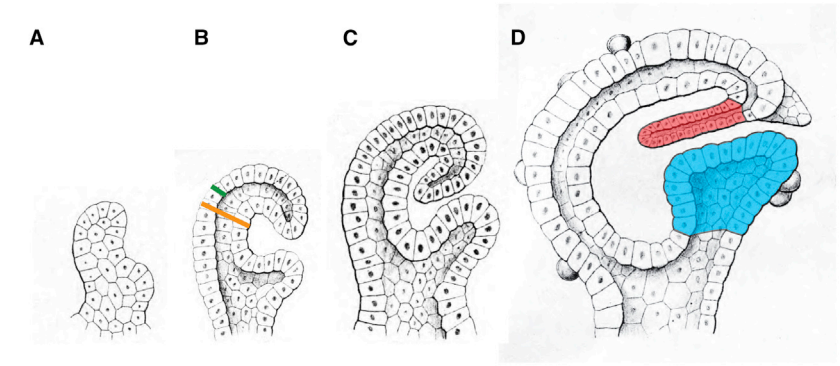

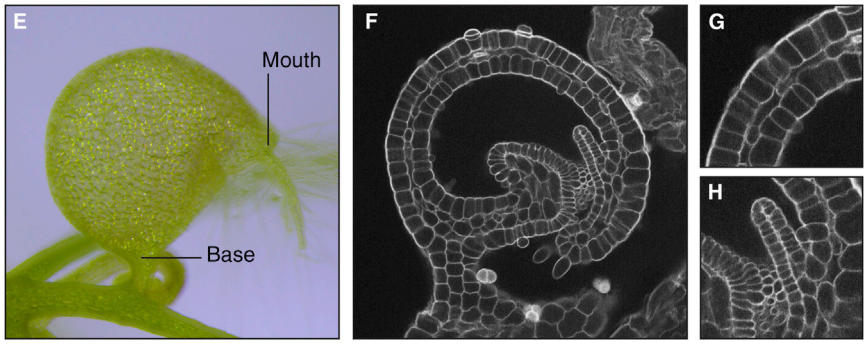

Figure 1. *Utricularia* undergoes a simple transition to three-dimensional growth.
(A–D) *Utricularia* invaginates to produce an enclosed cup-shaped trap (adapted from drawings of *U. vulgaris* in [87]). In (B), a single cell layer is marked in green and the trap wall is marked in orange, and in (D), the trap door is marked in red and threshold in blue. (E) The mature *U. gibba* trap is a hollow cup (mouth and base labelled). (F) Confocal microscopy of *U. gibba* shows a similar shape to *U. vulgaris*), and allows us to observe the cellular basis of trap morphology, for example the two cell layer thick trap wall (G) and trap door (H).

have the higher velocities (and point in the opposite sense). In both cases, however, growth rates within the tissue would be the same.

Velocities are therefore not a direct representation of growth. Instead, we need to take the spatial gradient of the velocity field (the rate of change in velocity with position) to calculate local growth rates and orientations. Rather than a vector, the outcome of this calculation is represented with another measure, termed a tensor [2,3] (Figure 2A). Tensors have multiple axes, each with an associated magnitude and orientation, but unlike vectors, tensors have no sense (their axes do not have arrowheads at one end). For three-dimensional growth, a tensor can be represented as an ellipsoid, with magnitudes along three orthogonal axes representing growth rates in three orientations. The greatest magnitude lies along the principal orientation of growth. The sum of the growth rates along all three axes gives the volumetric growth rate. For the case of isotropic growth, the tensor corresponds to a sphere (all magnitudes equal). For two-dimensional growth, the tensor can be represented with an ellipse and has only two axes, with the sum of growth rates along these axes corresponding to the areal growth rate. In addition, tensors may have a rotational component to describe how regions of tissue rotate relative to each other during growth [2]. As the growth tensor may vary from one position to another, a tensor field is needed to fully capture growth (Figure 2D). This raises the problem of how the growth tensor field of a deforming structure such as the *Utricularia* trap can be measured.

How Do We Measure Growth?

The growth tensor field can be described at many scales, from the subcellular to the tissue. The most direct way to estimate growth is by tracking the movement of landmarks on a developing structure. In *Nitella axillaris*, subcellular growth rates have been tracked by marking the cell surface with ink spots and following their movement throughout development [4]. In bacterial cells, subcellular growth can also be estimated by imaging the incorporation of fluorescently labelled cell wall components [5]. This work has revealed a range of growth patterns, from growth localised entirely to one region of the cell, to the intercalation of wall components throughout the cell. But unlike bacteria, where growth is directly coupled to the incorporation of new wall monomers, plant cell walls extend by wall loosening without the necessary addition of new components [6]. Therefore, it may be difficult to observe subcellular growth in plant cells by imaging the incorporation of cell wall components.

Landmarks for tracking growth of a multicellular tissue, such as the *Utricularia* trap (Figure 1), include cell vertices, air pores, trichomes and adhesive fluorescent particles [7–11]. Components of the growth tensor, such as growth rate or principal orientations of growth, can then be displayed. The growth tensors of individual cells can also be estimated [12,13], allowing a cellular growth tensor field to be visualised (where each tensor derives from a cell). In many cases, growth is described in two-dimensions, but the epidermal layer of the *Arabidopsis* meristem has been live-imaged in three dimensions [13–16]. Live imaging complex volumes in three dimensions is a challenge, because of the depth of imaging required and occlusion by other structures (for example, sepals surrounding petals). The *Utricularia* trap has the advantage that it is only two cells thick and is not surrounded by other tissues for much of its development.

Another way to estimate growth is through clonal analysis. Here a heritable change is induced in individual cells of a tissue, usually a change in pigment or in the expression of a fluorescent protein [7,17]. The plant is imaged after several rounds of cell division, after which the area, shape and number of cells in the resulting clones can be determined. For example, clones of GFP-expressing cells induced in *Utricularia gibba* reveal a range of clone sizes and shapes after three days of growth (Figure 3). Growth may be inferred by comparing the size and shape of the initial cell to the same measures for the final clone. But as detailed information about the initial cell is usually lacking, a statistical approach, with assumptions about average initial cell configurations, is typically needed to infer components of

A

Concept	Example	Properties	Visualisation
Scalar	Concentration Temperature	Magnitude	Single number
Vector	Polarity Velocity Force	Magnitude Axis (orientation) Sense (direction)	
Tensor	Stress Growth	Magnitudes (2 in 2D, 3 in 3D) Axes (2 in 2D 3 in 3D) Rotation	

B

1.1	1.1	1.1	1.1	1.1
1.0	1.0	1.0	1.0	1.0
0.9	0.9	0.9	0.9	0.9
0.8	0.8	0.8	0.8	0.8

C

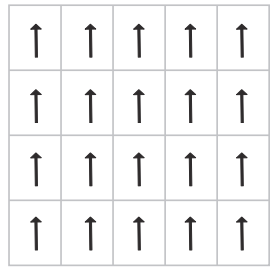

D

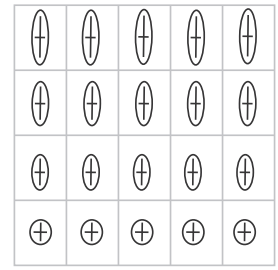

Current Biology

Figure 2. Key concepts in plant growth.
(A) Summary of concepts key to understanding plant growth. In development, measures—growth, polarity, stress and so on—may vary across a tissue. Depending on what is being measured, this may correspond to: (B) a scalar field, for example a field of concentrations; (C) a vector field, for example a field of polarities; or (D) a tensor field, for example a field of growth tensors. In (B), concentration increases from the bottom to the top. In (C), polarity at each position points upwards. As polarity conveys only axis and direction, the magnitude of the vector can be considered as constant (set to unit length). In (D), growth tensors are isotropic at the bottom and gradually become more anisotropic towards the top. For anisotropic growth, the principal orientation of growth is vertical.

the growth tensor. Clonal analysis has been used to infer growth patterns in a wide variety of plant tissues including the *Arabidopsis* leaf and petal [7,18]. It has also been applied to complex three-dimensional structures such as the *Antirrhinum majus* corolla [19], and the *Arabidopsis* gynoecium [20] and meristem [21]. In the flower and gynoecium, only surface sectors were used to determine the pattern of growth, whereas in the meristem, sectors throughout the entire volume were used to assess growth rates volumetrically [21].

Estimating components of the growth tensor field by these methods gives a description of growth, but begs the question of how the observed growth tensor field is generated. Plant tissues are congregations of cells. The growth rate of a cell in isolation depends on both cell wall extensibility and cell turgor. Turgor supplies the force (pressure) for growth and puts the cell wall under tension. The rate of growth depends on the extensibility of the wall in yielding to this pressure [22]. Higher turgor or wall extensibility promote faster growth. Cellular growth can be isotropic (the same along all axes) or anisotropic (higher along some axes). Turgor acts isotropically whereas cell wall extensibility can be anisotropic.

Specified and Resultant Growth

For an isolated plant cell, growth depends solely on patterns of wall extensibility and level of turgor for that cell. However, cells within a tissue are connected and each cell may be constrained by its neighbours, influencing how it grows. Here it is useful to divide growth into two types: specified and resultant. Specified growth is how a region (a cell in this case) would grow in isolation (due to its own turgor and wall extensibility), whereas resultant growth is how the cell grows when mechanical constraints of neighbouring regions are taken into account [23,24]. These mechanical constraints can alter the rates and orientations of a cell's growth and introduce rotations.

Thus, whereas specified growth refers to the active growth properties of a cell, resultant growth also includes passive effects brought about by contacts with neighbours. Specified growth and resultant growth are both tensors. The specified growth tensor comprises growth rates along different axes but has no rotational component (we assume the cell has no intrinsic rotational force that would make it turn in isolation). The resultant growth tensor may have rotational components (the cell may turn in relation to the tissue) and the rates and orientations of resultant growth may not be identical to those of the specified growth tensor, due to the constraints of neighbouring regions. To understand three-dimensional morphogenesis, including the generation of curvature, we therefore need to know how patterns of specified growth are controlled and how mechanical constraints lead to observed patterns of resultant growth.

For a given tissue, we may distinguish between two types of constraints or forces that can contribute to tissue deformation: external and internal. In both cases, the forces derive from cells pulling or pushing on each other, but in one case (external) the cells interact through epidermal walls that come into secondary contact (requiring collision detection from a modelling perspective).

External Forces

Some of the constraints on growth may originate externally to the tissue under consideration. For example, you can bend a thin flat strip of metal into an arc by pressing at both ends. External forces can play a similar role during development. In the cotton flower bud, the petals are linked together by entangled trichomes, causing the petals to pull against each other as they grow. These forces cause the petals to bend into a curve that encloses the internal organs [25]. If trichomes are not present, petals become twisted instead of forming a smooth curve.

Even though the push and pull of one organ against another is likely common in development, such forces are not always involved in driving deformations in three dimensions. For example, different organ whorls in the flower are in close contact and may apply forces upon one other, yet mutants that modify floral organ identities do not have strong effects on the shape

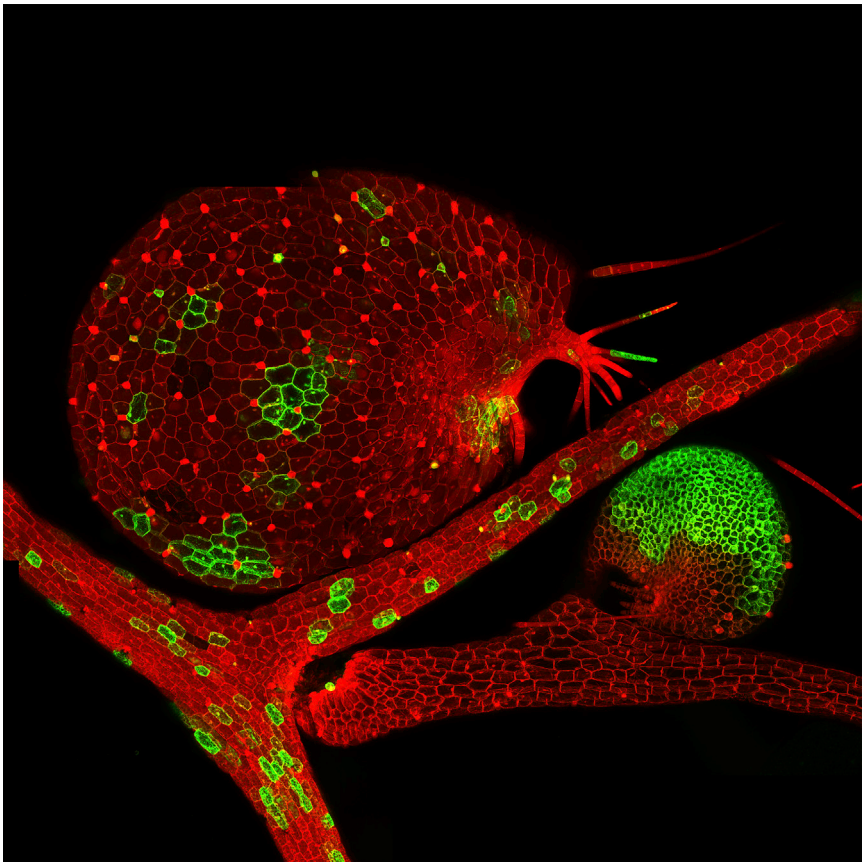

Figure 3. GFP-expressing sectors in *Utricularia gibba* traps.
Sector shapes and sizes (in green) in transgenic *U. gibba* vary across a trap (large trap on left) and between different developmental stages (left and right). Sectors of GFP expression were generated by heat-shock induction of a Cre recombinase, which led to recombination and activation of GFP expression [88]. Image was taken three days after heat shock.

of adjacent organs [26]. *A. majus* petals, which develop a complex three-dimensional shape, appear normal in mutants with homeotically transformed stamens [27]. Shaping of the *Utricularia* trap is also unlikely to derive solely from external forces as it is not surrounded by other tissues for much of its development. This suggests that in many cases something other than external forces shapes development in three dimensions.

Tissue Conflict Resolution

If specified growth rates vary across a tissue, there can be a potential conflict between nearby regions trying to grow in different ways. Such conflicts can cause stresses (derived from internal forces) and resultant anisotropy in areas where fast and slow growing regions meet. A region may be passively stretched in one orientation by a fast-growing neighbouring region, or passively constrained in one orientation by a slower-growing neighbouring region. For some specified growth patterns, such potential conflicts may be partially or fully resolved through local rotations, giving curvature or bending (evident in the rotational components of the resultant growth tensor). In a tissue sheet, these rotations may be in or out of plane. Out-of-plane rotations, for example, occur when a sheet buckles and forms a three-dimensional curve or cup. For the development of three-dimensional shape, this means that it is possible to produce a three-dimensional structure (a curved sheet) through growth patterns specified in only two dimensions.

This mechanism for generating rotations within or out of the plane is called tissue conflict resolution, and has been divided into three types [28,29]: areal, surface and directional (discussed further in [28]). In areal conflict, different regions of a sheet have different specified areal growth rates, whereas in surface conflict, the two surfaces of a sheet have different specified growth rates. Areal conflict plays a role in generating curvature of lily petals [30] and leaves of *cincinnata* mutants in *A. majus*, where enhanced growth at the margin causes a wavy edge [31]. With directional conflict, specified growth orientations vary across a tissue. For example, in the *A. majus* petal, an orthogonal pattern of specified growth orientations is thought to contribute to curvature [29].

The above examples illustrate tissue conflict resolution within a sheet, but the same principles apply to tissue volumes. In this case, surface and areal conflict can both be considered as regional conflicts, where different tissue regions have different specified growth rates. Directional conflict has the further complication in three compared to two dimensions, that an additional growth orientation needs be considered.

Cellular Basis of Anisotropy

Directional conflict and coordinated patterns of oriented growth require a mechanism for specified growth to be anisotropic. At the cellular level, specified anisotropy derives from anisotropic cell wall properties: greater extensibility of cell walls in some orientations compared to others. Directional cell wall reinforcement depends on cellulose fibres in the wall [32]. The fibres are relatively inextensible along their length, and as the cell expands, the path of least resistance is to pull the fibres apart (widening the gap between fibres). If cellulose fibres are aligned in one orientation, the cell wall is therefore more extensible in the perpendicular orientation and will preferentially expand along that axis.

The alignment of cellulose fibres themselves is determined by microtubule alignments [33]. These provide tracks that direct the cellulose synthase complex, and create cellulose alignments in parallel with the underlying microtubules [34,35]. The pattern of microtubule alignments within a cell thus provides a mechanism for guiding cell wall anisotropy. In the *Arabidopsis* hypocotyl, after initial pectin loosening, microtubule orientation changes to create anisotropic side walls and promote anisotropic growth [36]. Different faces of a cell can have different arrangements of

microtubules and cellulose fibres [37], which may contribute to the pattern of specified anisotropic growth. However, the details by which cellulose fibre alignments on different faces are related to specified growth patterns are still poorly understood [22].

To specify anisotropic growth, a cell must be able to distinguish axes (have axiality) so that cellulose alignments can be oriented with respect to them. To specify organ-wide axiality fields, the axiality of cells must be coordinated across a tissue. In plants two means have been proposed to coordinate this axiality field: stresses [12,38] and polarity [23].

Stresses

In a tissue where specified growth is isotropic, stress patterns can be modulated by tissue geometry, external forces acting on the tissue, and differential specified growth rates. The stress hypothesis suggests that a cell can sense the principal orientation of stresses and orient specified growth in relation to them. This hypothesis is particularly attractive because stress, like growth, is a tensor (Figure 2A), which means that it could be used to directly specify aspects of growth. Ablating a cell in a plant tissue causes the microtubules of neighbouring cells to align with the principal orientation of stress around the ablated cell [38], suggesting that stress may promote anisotropic cell wall reinforcement in parallel with the stress. Such reinforcement could give specified anisotropic growth perpendicular to the stress.

A global field of principal stress orientations could, in principle, coordinate specified growth anisotropies across an organ. Computational modelling has been used to predict global patterns of principal stress orientations that are due to tissue geometry in the *Arabidopsis* meristem, considered as a pressurised cylinder [38]. Microtubules form supracellular alignments in parallel with the predicted stress field, suggesting that a global stress field may be coordinating specified cellular anisotropy via microtubule orientation. Stresses have also been used in a computational model of the *Arabidopsis* sepal to orient specified anisotropy [12]. In this case, a global stress field is proposed to arise from differential specified isotropic growth rates (areal tissue conflict) rather than tissue geometry. The global stress field needs to be maintained in the face of cells modifying their specified growth in relation to local stresses. To achieve this, it has been proposed that cells may be able to sense average stress across the tissue to orient growth [12], but how this averaging occurs, or how local and global stresses can be distinguished is unclear.

Polarity

A second hypothesis for the control of specified anisotropic growth is that each cell has a polarity (unit vector, Figure 2A) and the axiality component of this vector can be used to specify anisotropic growth orientation. Other components of the specified growth tensor can be provided separately; for example, growth regulators determine the values of specified growth rates parallel and perpendicular to a polarity axis.

In support of the polarity hypothesis, several asymmetrically localised proteins (proteins preferentially localised at one end of the cell) have been described for plant cells, such as PINs [39], BASL [40] and ROPs [41]. These protein distributions provide each cell with a vector (polarity). Such cellular polarity can be coordinated across a tissue, as exemplified by the PIN family of auxin transporters in *Arabidopsis* leaf and petal primordia [7,18]. This tissue-wide coordination of cellular polarities can be represented as a vector (polarity) field. Several models have been proposed using auxin to explain the ability of PINs to form coordinated polarity fields across a tissue [42–47]. In all of these models, polarity fields can be modified by the position of auxin sources and sinks.

Given a polarity field, cell wall properties could be altered to specify anisotropic growth in relation to that field. This may involve biasing the alignments of microtubules towards certain orientations with respect to the axis of polarity, or loosening cell walls parallel or perpendicular to the polarity axis. A difference between the polarity and the stress field hypotheses is that with the polarity hypothesis it is possible to orient growth either parallel or perpendicular to polarity, whereas with the stress field hypothesis microtubules typically align parallel to the principal orientation of tension [12,38]. A further complication with the stress hypothesis is that cell wall reinforcement feeds back to modify stresses: reinforcement in the direction of stress (tension) reduces the stress by creating a greater cross-sectional area of cellulose fibres resisting the stress (stress is force divided by cross-sectional area of resisting material). By contrast, polarity fields allow orientations to be specified independently of stresses generated. Thus, while the stress hypothesis is attractive because it directly exploits stresses within the tissue, the polarity hypothesis allows for greater developmental flexibility.

It has also been proposed that stresses may themselves provide information to establish or guide cell polarity [48,49]. However, stress is a tensor and therefore does not carry information about sense (the orientations have no arrowheads, Figure 2A, D). Thus, it is not possible for the orientation of stresses alone to determine polarity. Rather, a gradient of stresses is needed to specify polarity, much in the manner of a graded molecular concentration [48].

Genetic Modulation of Growth

Whichever of the above mechanisms for specifying growth apply, they should allow modulation of growth through the action of genes. The role of genes in modifying three-dimensional shape has been primarily investigated by analysing mutants with altered shapes. These include floral mutants in *A. majus* that produce spurs [50] or exhibit disrupted floral symmetry [51], fruit shape mutants in squash, brassicas and tomato [20,52,53], and meristem shape mutants in *Arabidopsis* [54–56]. There are also mutants where flat leaves have been transformed into cup shapes [57] or three-dimensional structures with wavy edges [31].

A clear example of a mutation affecting a simple three-dimensional shape is one that affects the *Arabidopsis* sepal. The mature wild-type sepal bends out of plane into a near cup-shape [58]. This curvature may arise through areal conflict, with the centre of the sepal being specified to grow faster than the margins. The *Igo* mutant does not exhibit this curvature, a defect associated with a reduction in the number of giant cells in the centre of the sepal [58].

For more complex three-dimensional shapes it is difficult to make clear links between the mutant phenotype and the effect of genes on growth, as many possible specified growth patterns may cause similar resultant growth patterns. For instance, in the *Utricularia* trap (Figure 1), the bending of the trap wall into a curve may be caused by surface conflict, areal conflict, and/or directional conflict. In complex cases like this, computational

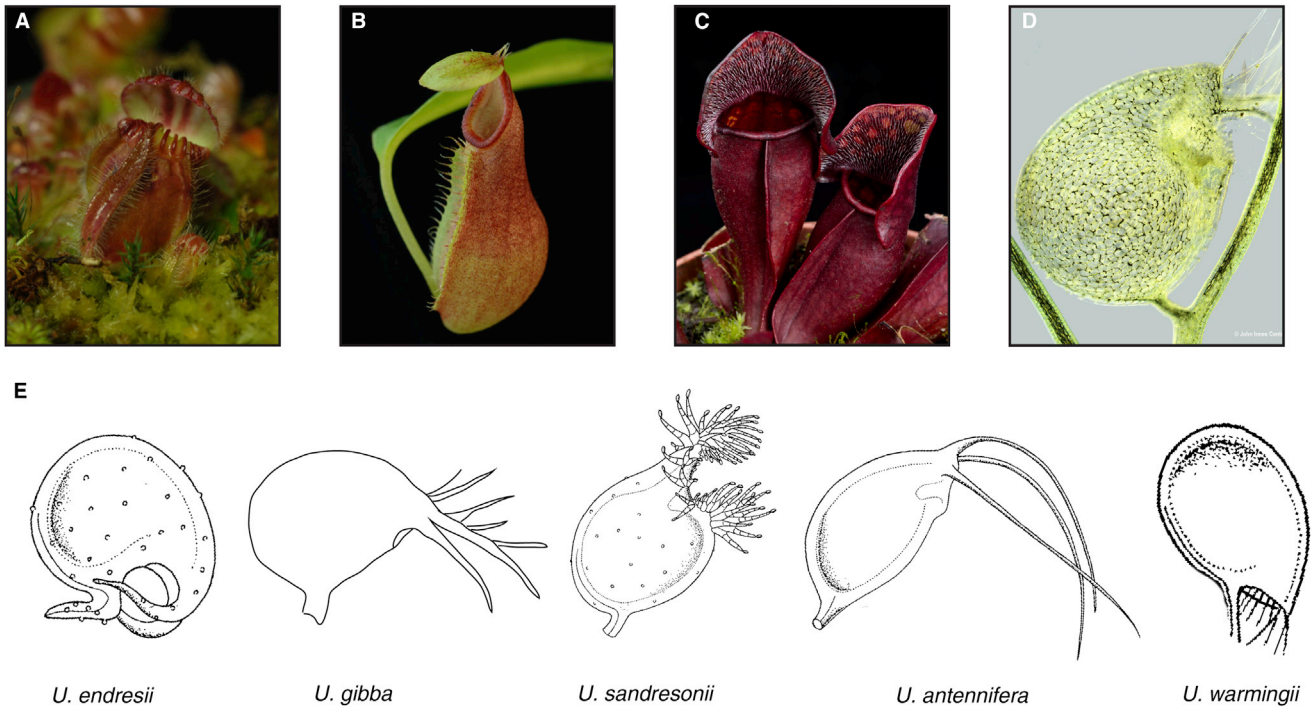

Figure 4. Evolution of cup-shaped traps in carnivorous plants.
Cup-shaped traps have evolved from flat leaves four times independently: in the Cephalotaceae (A), Nepenthaceae (B), Sarraceniaceae (C) and Lentibulariaceae (D). Within the Lentibulariaceae, the genus *Utricularia* contains species with a diversity of trap shapes (E). Diagrams of *Utricularia* traps apart from *U. gibba* are adapted from [86]. © Board of Trustees of the Royal Botanic Gardens, Kew.

modelling is required to bridge the gap between specified and resultant growth, to predict how changes in gene function might affect morphogenesis of a connected tissue.

A range of computational models have been used to understand plant form (summarised in [59,60]). The majority consider plant organs as sheets. These include models at the tissue-level (of leaves [7,61,62], sepals [12] and petals [18]), and at the cellular level [63,64]. These models use different ways to orient specified anisotropic growth; by polarity [7,18], stresses [12], or in parallel with veins [62]. Genes may be integrated within these models as components that modulate specified growth parameters. For example, *JAGGED* was assigned a role in promoting growth and modulating polarity in a model of *Arabidopsis* petal development [18].

Computational models of three-dimensional structures have been developed. These either consider a tissue as a sheet deforming in three dimensions [19,20,29] or as a volume (such as the *Arabidopsis* meristem or organ primordium). The approach taken depends on which stage in development is being modelled, as organs tend to begin as volumes and become more sheet-like (see Figure 1A–D, for example, in *Utricularia*). For the *A. majus* corolla, out-of-plane deformation of a sheet was proposed to arise by the *DIVARICATA* gene modifying anisotropic growth in relation to a polarity field [29]. The *Arabidopsis* gynoecium has also been modelled in a similar manner in relation to the gene *FRUITFULL* [20].

Three-dimensional structures have also been modelled by considering sequential two-dimensional sections. For example, the pitcher trap of *Sarracenia purpurea* has been modelled as two cross sections — one of the trap hollow and another of the adaxial ridge that forms the bottom lip of the trap [65]. The authors propose that a switch in cell division plane is sufficient to drive a change in orientation of anisotropic growth. However, it is unclear how the plane of division (which reflects how a cell becomes partitioned), determines specified growth orientation of a cell (which depends on the extensibility of all walls). Also, a disadvantage of modelling separate sections is that mechanical interactions through tissue connectivity are not considered.

The control of *Arabidopsis* meristem shape has also been analysed genetically [66,67] and in terms of growth [68] and cell division patterns [69]. It has been modelled as a sheet-like dome and these models can accurately predict phyllotactic patterns [44,70] and gene expression patterns of meristem shape mutants [71]. Volumetric cellular models of the *Arabidopsis* shoot apical meristem and embryo have also been recently developed [24,72]. These models consider how genes control turgor pressure and cell wall loosening to drive organogenesis, though the contribution of specified anisotropy is less explored. The embryo model involves isotropic specified growth, while in the meristem model the orientation of anisotropic growth is specified by an external field, rather than by an internal pattern of stresses or polarity [72]. The embryo model shows how genes promoting cell division may slow down growth, as more cell walls provide greater resistance to the expansive force of turgor [24].

Evolution of Three-Dimensional Shapes

The above studies show how the combination of computational modelling with developmental, growth and genetic analysis is

helping us understand how three-dimensional shapes are formed. These advances also provide a way to study how three-dimensional shapes have evolved and diversified.

The evolution of shoot meristems—apical structures that generate volumetric tissues—is thought to have occurred both during the transition to land and within aquatic plants [73]. Prior to this, algal ancestors grew as filaments or planar structures, as charophyte algae do today [74,75]. The moss *Physcomitrella patens* undergoes a similar developmental switch from filamentous to meristematic growth [76], and has been used to analyse the genetic and developmental basis of the transition. Mutants have been isolated that are disrupted in meristem formation [77,78], and the combination of genetics, developmental analysis and computational modelling is likely to provide mechanistic insights into how three-dimensional growth arose in land plants.

A striking feature of plant shape is that similar forms can evolve independently. This applies to meristems, which evolved independently in land plants and in brown algae [73], and also for many shapes within land plants. For example, cup-shaped traps evolved from relatively flat leaves four times independently (Figure 4A–D) [79–81]. It is not clear whether genetic networks in plants with flat leaves were simply modulated in the transition to three dimensions, or whether novel regulators were recruited [65]. Carnivorous plant species such as *U. gibba* and *Cephalotus follicularis* both have flat leaves and traps on the same plant, and analysis of differences in gene expression between these structures has begun to address the question of how flat and cup-shaped leaves are related [82]. The combination of such approaches with computational modelling and developmental genetic analysis should allow us to understand the basis of the evolutionary transition of flat sheets to more complex tissue folds.

In addition to major shape differences among taxa, numerous variations in shape are present within single genera [83,84]. For example, the genus *Utricularia* contains over 200 species [85,86] that show substantial variation of trap size and shape (Figure 4E). A key question is how changes in gene activity and specified growth patterns lead to these variations. In the Brassicaceae, varying parameters can explain interspecies differences in gynoecium morphology [20]. The extension of this approach to other species, such as *Utricularia*, will allow us to determine the genetic controls underlying further interspecies differences in three-dimensional form.

Conclusions

Genes influence plant morphogenesis by modifying the rates and orientations of specified growth. The mechanical connectivity of cells introduces constraints that can lead to tissue buckling, bulging and bending in three dimensions. Computational modelling is helping us understand the mechanistic link between gene activity and morphogenesis by allowing us to formulate hypotheses for how patterns of specified growth are established, and how they may lead to resultant deformations. However, many of the molecular and physical mechanisms that connect cell and tissue level behaviours remain to be uncovered. As well as established model systems, new systems such as *Utricularia,* which has the advantage of convenient imaging and few cell layers, provide an opportunity to address these problems and give a full understanding of how genes modulate growth to generate the diversity of three-dimensional plant forms.

ACKNOWLEDGEMENTS

We thank all the members of the Coen lab for helpful discussions. Thanks to Desmond Bradley, Beatriz Gonçalves, Karen Lee, Catherine Mansfield, Jake Newman and Annabel Whibley for comments on the manuscript. Special thanks to Minlong Cui for transgenic *Utricularia gibba* and to Claire Bushell, Karen Lee, Andrew Davis and Patrick Diaz for the images in Figures 3 and 4.

REFERENCES

1. Menshykau, D., Blanc, P., Unal, E., Sapin, V., and Iber, D. (2014). An interplay of geometry and signaling enables robust lung branching morphogenesis. Development *141*, 4526–4536.
2. Hejnowicz, Z., and Romberger, J.A. (1984). Growth tensor of plant organs. J. Theor. Biol. *110*, 93–114.
3. Richards, O.W., and Kavanagh, A. (1943). The analysis of the relative growth gradients and changing form of growing organisms: illustrated by the tobacco leaf. Am. Nat. *77*, 385–399.
4. Green, P.B. (1954). The spiral growth pattern of the cell wall in Nitella axillaris. Am. J. Bot. *41*, 403.
5. Kuru, E., Tekkam, S., Hall, E., Brun, Y.V., and VanNieuwenhze, M.S. (2015). Synthesis of fluorescent D-amino acids and their use for probing peptidoglycan synthesis and bacterial growth in situ. Nat. Protoc. *10*, 33–52.
6. Cosgrove, D.J. (2005). Growth of the plant cell wall. Nat. Rev. Mol. Cell Biol. *6*, 850–861.
7. Kuchen, E., Fox, S., de Reuille, P.B., Kennaway, R., Bensmihen, S., Avondo, J., Calder, G.M., Southam, P., Robinson, S., Bangham, A., *et al*. (2012). Generation of leaf shape through early patterns of growth and tissue polarity. Science *335*, 1092–1096.
8. Solly, J.E., Cunniffe, N.J., and Harrison, C.J. (2017). Regional growth rate differences specified by apical notch activities regulate liverwort thallus shape. Curr. Biol. *27*, 16–26.
9. Remmler, L., and Rolland-Lagan, a.-G. (2012). Computational method for quantifying growth patterns at the adaxial leaf surface in three dimensions. Plant Physiol. *159*, 27–39.
10. Dumais, J., and Kwiatkowska, D. (2002). Analysis of surface growth in shoot apices. Plant J. *31*, 229–241.
11. Armour, W.J., Barton, D.A., Law, A.M., and Overall, R.L. (2015). Differential growth in periclinal and anticlinal walls during lobe formation in arabidopsis cotyledon pavement cells. Plant Cell *27*, 2484–2500.
12. Hervieux, N., Dumond, M., Sapala, A., Routier-Kierzkowska, A.L., Kierzkowski, D., Roeder, A.H.K., Smith, R.S., Boudaoud, A., and Hamant, O. (2016). A mechanical feedback restricts sepal growth and shape in Arabidopsis. Curr. Biol. *26*, 1019–1028.
13. Louveaux, M., Julien, J.-D., Mirabet, V., Boudaoud, A., and Hamant, O. (2016). Cell division plane orientation based on tensile stress in Arabidopsis thaliana. Proc. Natl. Acad. Sci. USA, 201600677.
14. Reddy, G.V., Heisler, M.G., Ehrhardt, D.W., and Meyerowitz, E.M. (2004). Real-time lineage analysis reveals oriented cell divisions associated with morphogenesis at the shoot apex of Arabidopsis thaliana. Development *131*, 4225–4237.
15. Serrano-Mislata, A., Schiessl, K., and Sablowski, R. (2015). Active control of cell size generates spatial detail during plant organogenesis. Curr. Biol. *25*, 2991–2996.
16. Barbier de Reuille, P., Routier-Kierzkowska, A.-L., Kierzkowski, D., Bassel, G.W., Schüpbach, T., Tauriello, G., Bajpai, N., Strauss, S., Weber, A., Kiss, A., *et al*. (2015). MorphoGraphX: A platform for quantifying morphogenesis in 4D. Elife *4*, 5864.

17. Poethig, R.S., and Sussex, I.M. (1985). The cellular parameters of leaf development in tobacco: a clonal analysis. Planta *165*, 170–184.

18. Sauret-Güeto, S., Schiessl, K., Bangham, A., Sablowski, R., and Coen, E. (2013). JAGGED controls Arabidopsis petal growth and shape by interacting with a divergent polarity field. PLoS Biol. *11*, e1001550.

19. Green, A.A., Kennaway, J.R., Hanna, A.I., Andrew Bangham, J., and Coen, E. (2010). Genetic control of organ shape and tissue polarity. PLoS Biol. *8*, e1000537.

20. Eldridge, T., Ł, Ł., Stacey, N., Jantzen, F., Moubayidin, L., Sicard, A., Southam, P., Kennaway, R., Lenhard, M., Coen, E.S., *et al*. (2016). Fruit shape diversity in the Brassicaceae is generated by varying patterns of anisotropy. Development *143*, 3394–3406.

21. Bencivenga, S., Serrano-Mislata, A., Bush, M., Fox, S., and Sablowski, R. (2016). Control of oriented tissue growth through repression of organ boundary genes promotes stem morphogenesis. Dev. Cell *39*, 198–208.

22. Cosgrove, D.J. (2016). Catalysts of plant cell wall loosening. F1000Research *5*, 1–13.

23. Kennaway, R., Coen, E., Green, A., and Bangham, A. (2011). Generation of diverse biological forms through combinatorial interactions between tissue polarity and growth. PLoS Comput. Biol. *7*, e1002071.

24. Bassel, G.W., Stamm, P., Mosca, G., Barbier de Reuille, P., Gibbs, D.J., Winter, R., Janka, A., Holdsworth, M.J., and Smith, R.S. (2014). Mechanical constraints imposed by 3D cellular geometry and arrangement modulate growth patterns in the Arabidopsis embryo. Proc. Natl. Acad. Sci. USA *111*, 8685–8690.

25. Tan, J., Walford, S.-A., Dennis, E.S., and Llewellyn, D. (2016). Trichomes control flower bud shape by linking together young petals. Nat. plants. *2*, 16093.

26. Coen, E.S., and Meyerowitz, E.M. (1991). The war of the whorls: genetic interactions controlling flower development. Nature *353*, 31–37.

27. Bradley, D., Carpenter, R., Sommer, H., Hartley, N., and Coen, E. (1993). Complementary floral homeotic phenotypes result from opposite orientations of a transposon at the plena locus of antirrhinum. Cell *72*, 85–95.

28. Coen, E., and Rebocho, A.B. (2016). Resolving conflicts: modeling genetic control of plant morphogenesis. Dev. Cell *38*, 579–583.

29. Rebocho, A.B., Southam, P., Kennaway, J.R., Bangham, J.A., and Coen, E. (2017). Generation of shape complexity through tissue conflict resolution. eLife *6*, e20156.

30. Liang, H., and Mahadevan, L. (2011). Growth, geometry, and mechanics of a blooming lily. Proc. Natl. Acad. Sci. USA *108*, 5516–5521.

31. Nath, U., Crawford, B., Carpenter, R., and Coen, E. (2003). Genetic control of surface curvature. Science *299*, 1404.

32. Baskin, T.I. (2005). Anisotropic expansion of the plant cell wall. Annu. Rev. Cell Dev. Biol. *21*, 203–222.

33. Paredez, A.R., Somerville, C., and Ehrhardt, D. (2006). Visualization of cellulose synthase with microtubules. Science *312*, 1491–1495.

34. Gutierrez, R., Lindeboom, J.J., Paredez, A.R., Emons, A.M.C., and Ehrhardt, D.W. (2009). Arabidopsis cortical microtubules position cellulose synthase delivery to the plasma membrane and interact with cellulose synthase trafficking compartments. Nat. Cell Biol. *11*, 797–806.

35. Chan, J., Crowell, E., Eder, M., Calder, G., Bunnewell, S., Findlay, K., Vernhettes, S., Höfte, H., and Lloyd, C. (2010). The rotation of cellulose synthase trajectories is microtubule dependent and influences the texture of epidermal cell walls in Arabidopsis hypocotyls. J. Cell Sci. *123*, 3490–3495.

36. Peaucelle, A., Wightman, R., and Höfte, H. (2015). The control of growth symmetry breaking in the Arabidopsis hypocotyl. Curr. Biol. *25*, 1746–1752.

37. Chan, J., Eder, M., Crowell, E.F., Hampson, J., Calder, G., and Lloyd, C. (2011). Microtubules and CESA tracks at the inner epidermal wall align independently of those on the outer wall of light-grown Arabidopsis hypocotyls. J. Cell. Sci. *124*, 1088–1094.

38. Hamant, O., Heisler, M.G., Jönsson, H., Krupinski, P., Uyttewaal, M., Bokov, P., Corson, F., Sahlin, P., Boudaoud, A., Meyerowitz, E.M., *et al*. (2008). Developmental patterning by mechanical signals in Arabidopsis. Science *322*, 1650–1655.

39. Friml, J., Vieten, A., Sauer, M., Weijers, D., Schwarz, H., Hamann, T., Offringa, R., and Jürgens, G. (2003). Efflux-dependent auxin gradients establish the apical-basal axis of Arabidopsis. Nature *426*, 147–153.

40. Robinson, S., Barbier de Reuille, P., Chan, J., Bergmann, D., Prusinkiewicz, P., and Coen, E. (2011). Generation of spatial patterns through cell polarity switching. Science *333*, 1436–1440.

41. Molendijk, A.J., Bischoff, F., Rajendrakumar, C.S., Friml, J., Braun, M., Gilroy, S., and Palme, K. (2001). Arabidopsis thaliana Rop GTPases are localized to tips of root hairs and control polar growth. EMBO J. *20*, 2779–2788.

42. Abley, K., De Reuille, P.B., Strutt, D., Bangham, A., Prusinkiewicz, P., Marée, A.F.M., Grieneisen, V.a, and Coen, E. (2013). An intracellular partitioning-based framework for tissue cell polarity in plants and animals. Development *140*, 2061–2074.

43. Abley, K., Sauret-Güeto, S., Marée, A.F., and Coen, E. (2016). Formation of polarity convergences underlying shoot outgrowths. eLife *5*, e18165.

44. Jönsson, H., Heisler, M.G., Shapiro, B.E., Meyerowitz, E.M., and Mjolsness, E. (2006). An auxin-driven polarized transport model for phyllotaxis. Proc. Natl. Acad. Sci. USA *103*, 1633–1638.

45. Rolland-Lagan, A.G., and Prusinkiewicz, P. (2005). Reviewing models of auxin canalization in the context of leaf vein pattern formation in Arabidopsis. Plant J. *44*, 854–865.

46. Feugier, F.G., Mochizuki, A., and Iwasa, Y. (2005). Self-organization of the vascular system in plant leaves: Inter-dependent dynamics of auxin flux and carrier proteins. J. Theor. Biol. *236*, 366–375.

47. Stoma, S., Lucas, M., Chopard, J., Schaedel, M., Traas, J., and Godin, C. (2008). Flux-based transport enhancement as a plausible unifying mechanism for auxin transport in meristem development. PLoS Comput. Biol. *4*, e1000207.

48. Heisler, M.G., Hamant, O., Krupinski, P., Uyttewaal, M., Ohno, C., Jönsson, H., Traas, J., and Meyerowitz, E.M. (2010). Alignment between PIN1 polarity and microtubule orientation in the shoot apical meristem reveals a tight coupling between morphogenesis and auxin transport. PLoS Biol. *8*, e1000516.

49. Bringmann, M., and Bergmann, D.C. (2017). Tissue-wide mechanical forces influence the polarity of stomatal stem cells in Arabidopsis. Curr. Biol. *27*, 877–883.

50. Golz, J.F., Keck, E.J., and Hudson, A. (2002). Spontaneous mutations in KNOX genes give rise to a novel floral structure in Antirrhinum. Curr. Biol. *12*, 515–522.

51. Luo, D., Carpenter, R., Copsey, L., Vincent, C., Clark, J., and Coen, E. (1999). Control of organ asymmetry in flowers of Antirrhinum. Cell *99*, 367–376.

52. Sinnot, E.W. (1922). Inheritance of fruit shape in Cucurbita pepo. I. Bot. Gaz. *74*, 95–103.

53. Tanksley, S.D. (2009). The genetic, developmental, and molecular bases of fruit size in tomato and shape variation. Plant Cell *16*, 181–190.

54. Clark, S.E., Running, M.P., and Meyerowitz, E.M. (1993). CLAVATA1, a regulator of meristem and flower development in Arabidopsis. Development *119*, 397–418.

55. Clark, S.E., Running, M.P., and Meyerowitz, E.M. (1995). CLAVATA3 is a specific regulator of shoot and floral meristem development affecting the same processes as CLAVATA1. Development *121*, 2057–2067.

56. Kayes, J.M., and Clark, S.E. (1998). *CLAVATA2*, a regulator of meristem and organ development in *Arabidopsis*. Development *125*, 3843–3851.

57. Aida, M., Ishida, T., Fukaki, H., Fujisawa, H., and Tasaka, M., 2. (1997). Genes involved in organ separation in arabidopsis: an analysis of the cup-shaped cotyledon mutant. Plant Cell. Am. Soc. Plant Physiol. *9*, 841–857.

58. Roeder, A.H.K., Chickarmane, V., Cunha, A., Obara, B., Manjunath, B.S., and Meyerowitz, E.M. (2010). Variability in the control of cell division underlies sepal epidermal patterning in Arabidopsis thaliana. PLoS Biol. *8*, e1000367.

59. Prusinkiewicz, P., and Runions, A. (2012). Computational models of plant development and form. New Phytol. *193*, 549–569.

60. Prusinkiewicz, P., and Lindenmayer, A. (1990). The Algorithmic Beauty of Plants (New York: Springer-Verlag).

61. Bilsborough, G.D., Runions, A., Barkoulas, M., Jenkins, H.W., Hasson, A., Galinha, C., Laufs, P., Hay, A., Prusinkiewicz, P., and Tsiantis, M. (2011). Model for the regulation of Arabidopsis thaliana leaf margin development. Proc. Natl. Acad. Sci. USA *108*, 3424–3429.

62. Runions, A., Tsiantis, M., and Prusinkiewicz, P. (2017). A common developmental programme can produce diverse leaf shapes. New Phytol. http://dx.doi.org/10.1111/nph.14449.

63. Merks, R.M., Guravage, M., Inzé, D., and Beemster, G.T.S. (2011). VirtualLeaf: an open source framework for cell-based modeling of plant tissue growth and development. Plant Physiol. *155*, 656–666.

64. Shapiro, B.E., Meyerowitz, E.M., and Mjolsness, E. (2013). Using cellzilla for plant growth simulations at the cellular level. Front. Plant Sci. *4*, 408.

65. Fukushima, K., Fujita, H., Yamaguchi, T., Kawaguchi, M., Tsukaya, H., and Hasebe, M. (2015). Oriented cell division shapes carnivorous pitcher leaves of Sarracenia purpurea. Nat. Commun. *6*, 6450.

66. Schoof, H., Lenhard, M., Haecker, a, Mayer, K.F., Jürgens, G., and Laux, T. (2000). The stem cell population of Arabidopsis shoot meristems in maintained by a regulatory loop between the CLAVATA and WUSCHEL genes. Cell *100*, 635–644.

67. Gordon, S.P., Chickarmane, V.S., Ohno, C., and Meyerowitz, E.M. (2009). Multiple feedback loops through cytokinin signaling control stem cell number within the Arabidopsis shoot meristem. Proc. Natl. Acad. Sci. USA *106*, 16529–16534.

68. Kwiatkowska, D. (2008). Flowering and apical meristem growth dynamics. J. Exp. Bot. *59*, 187–201.

69. Willis, L., Refahi, Y., Wightman, R., Landrein, B., Teles, J., Huang, K.C., Meyerowitz, E.M., and Jönsson, H. (2016). Cell size and growth regulation in the Arabidopsis thaliana apical stem cell niche. Proc. Natl. Acad. Sci. USA *113*, E8238–E8246.

70. Smith, R.S., Guyomarc'h, S., Mandel, T., Reinhardt, D., Kuhlemeier, C., and Prusinkiewicz, P. (2006). A plausible model of phyllotaxis. Proc. Natl. Acad. Sci. USA *103*, 1301–1306.

71. Gruel, J., Landrein, B., Tarr, P., Schuster, C., Refahi, Y., Sampathkumar, A., Hamant, O., Meyerowitz, E.M., and Jo nsson, H. (2016). An epidermis-driven mechanism positions and scales stem cell niches in plants. Sci. Adv. *2*, e1500989–e1500989.

72. Boudon, F., Chopard, J., Ali, O., Gilles, B., Hamant, O., Boudaoud, A., Traas, J., and Godin, C. (2015). A computational framework for 3D mechanical modeling of plant morphogenesis with cellular resolution. PLoS Comput. Biol. *11*, e1003950.

73. Peaucelle, A., and Couder, Y. (2016). Fibonacci spirals in a brown alga [Sargassum muticum (Yendo) Fensholt] and in a land plant [Arabidopsis thaliana (L.) Heynh.]: a case of morphogenetic convergence. Acta Soc. Bot. Pol. *85*, 1–15.

74. Zimmermann, W. (1952). Main results of the Telome Theory. Palaeobotanist *1*, 456–470.

75. Harrison, C.J. (2016). Development and genetics in the evolution of land plant body plans. Phil. Trans. R. Soc. B. *372*, 20150490.

76. Harrison, C.J., Roeder, A.H.K., Meyerowitz, E.M., and Langdale, J.A. (2009). Local cues and asymmetric cell divisions underpin body plan transitions in the moss Physcomitrella patens. Curr. Biol. *19*, 461–471.

77. Perroud, P.-F., Demko, V., Johansen, W., Wilson, R.C., Olsen, O.-A., and Quatrano, R.S. (2014). Defective Kernel 1 (DEK1) is required for three-dimensional growth in Physcomitrella patens. New Phytol. *203*, 794–804.

78. Aoyama, T., Hiwatashi, Y., Shigyo, M., Kofuji, R., Kubo, M., Ito, M., and Hasebe, M. (2012). AP2-type transcription factors determine stem cell identity in the moss Physcomitrella patens. Development *3129*, 3120–3129.

79. Givnish, T.J. (2015). New evidence on the origin of carnivorous plants. Proc. Natl. Acad. Sci. USA *112*, 10–11.

80. Franck, D.H. (1976). The morphological interpretation of epiascidiate leaves: an historical perspective. Bot. Rev. *42*, 345–388.

81. Ellison, A.M., and Gotelli, N.J. (2009). Energetics and the evolution of carnivorous plants–Darwin's "most wonderful plants in the world". J. Exp. Bot. *60*, 19–42.

82. Fukushima, K., Fang, X., Alvarez-Ponce, D., Cai, H., Carretero-Paulet, L., Chen, C., Chang, T.-H., Farr, K.M., Fujita, T., Hiwatashi, Y., *et al*. (2017). Genome of the pitcher plant Cephalotus reveals genetic changes associated with carnivory. Nat. Ecol. Evol. *1*, 59.

83. Kramer, E.M., and Hodges, S.A. (2010). *Aquilegia* as a model system for the evolution and ecology of petals. Phil. Trans. R. Soc. Lond. B. Biol. Sci. *365*, 477–490.

84. Neale, S., Goodall-Copestake, W., and Kidner, C.A. (2006). The evolution of diversity in Begonia. In Floriculture, Ornamental and Plant Biotechnology: Advances and Topical Issues, pp. 276–277.

85. Fleischmann, A. (2012). The new utricularia species described since Peter Taylor's monograph. Carniv. Plant Newsl. *41*, 67–76.

86. Taylor, P. (1989). The genus Utricularia - a taxonomic monograph (Royal Botanic Gardens).

87. Meierhofer, H. (1902). Beitrage zur Anatomie und Entwickelungsgeschichte der Utricularia-Blasen. Flora *90*, 84–114.

88. Gallois, J.-L., Woodward, C., Reddy, G.V., and Sablowski, R. (2002). Combined SHOOT MERISTEMLESS and WUSCHEL trigger ectopic organogenesis in Arabidopsis. Development *129*, 3207–3217.